

# FZ crystal growth of monochromator-grade YB<sub>66</sub> single crystals as guided by topographic and double-crystal diffraction characterization

T. Tanaka<sup>a\*</sup>, Z. U. Rek<sup>b</sup>, Joe Wong<sup>c</sup>, M. Rowen<sup>b</sup>

<sup>a</sup> National Institute for Research in Inorganic Materials, Tsukuba, Ibaraki 305-0044, Japan

<sup>b</sup> Stanford Synchrotron Radiation Laboratory, P. O. Box 4349, Stanford, CA 94309, USA

<sup>c</sup> Lawrence Livermore National Laboratory, University of California, P.O. Box 808, Livermore, CA 94551, USA

E-mail: [tanaka.takaho@nims.go.jp](mailto:tanaka.takaho@nims.go.jp)

**Abstract.** YB<sub>66</sub> crystals grown with an indirect heating floating zone method were extensively characterized using a variety of X-ray diffraction techniques such as synchrotron white beam transmission and reflection topography, section topography and conventional double-crystal rocking curve measurements using Cu K $\alpha$  and Mg K $\alpha$  sources. The observed crystal defects and deformations were correlated with changes in the crystal growth process. The interplay between systematic characterization and process improvements results in the growth of high quality single crystals of YB<sub>66</sub> that can be used as an efficient element for monochromatization of synchrotron soft X-ray in the 1 - 2 keV energy range.

*Keywords:* YB<sub>66</sub>; Soft X-ray monochromator; Floating zone growth; X-ray diffraction characterization

## 1. Introduction

The unique covalent bonding of boron-rich borides makes it possible to form compounds having very complicated crystal structure. One such typical boron-rich boride is YB<sub>66</sub> whose crystal structure is a fcc lattice formed by super-icosahedra, each of which consists of thirteen B<sub>12</sub> icosahedra [1]. The unit cell of YB<sub>66</sub> contains 1584 boron atoms and only 24 yttrium atoms. Because of the complicated crystal structure, YB<sub>66</sub> behaves like an amorphous compound in phonon related properties such as, thermal conductivity, heat capacity and internal friction [2, 3, 4].

YB<sub>66</sub> has long been considered as a novel soft X-ray monochromator [5] to access the energy region 1-2 keV for synchrotron radiation, because of a large  $d$ -value ( $2d = 11.76$  Å) of its 4 0 0 reflection plane and superior material and X-ray properties. For this energy region, in fact, grating monochromators must be operated at extremely glancing angles so that high transmission and resolution cannot be achieved. Prior

to 1993 [6], no adequate monochromator crystal satisfied both X-ray and materials property requirements such as large d-spacing, high resolution and reflectivity, absence of intrinsic absorption of constituent elements, vacuum compatibility and toughness for radiation damage.

An international collaborative effort has for several years been devoted to develop the  $\text{YB}_{66}$  soft X-ray monochromator. The collaboration included: (a) growth of large and high quality single crystals of  $\text{YB}_{66}$  [7, 8, 9]; (b) systematic hard X-ray characterization with rocking curve measurements, and X-ray topography to map out sub-grain structure and growth-induced defects [10, 11]; (c) crystal reflectivity [12] and soft X-ray double-crystal rocking curve [6] measurements as a function of crystal growth parameters and position on a grown crystal and (d) evaluation of  $\text{YB}_{66}$  monochromator performance by XAFS measurements on selected Mg, Al and Si containing compounds [13]. Feedback loop between these characterization investigations, especially (b), and the crystal growth has been quite effective in improving and attaining growth of large and perfect enough crystals for monochromator application. The combined effort led to a successful installation of a double-crystal  $\text{YB}_{66}$  monochromator on the JUMBO beamline [14] at Stanford Synchrotron Radiation Laboratory (SSRL), which has been in operation since early 1993 [6]. In this paper we report a systematic study of the  $\text{YB}_{66}$  crystal growth process and crystal quality derived from topographic imaging and rocking curve measurements. The characterization results were used to advantage as guide for improving the crystal growth process to attain monochromator-grade of  $\text{YB}_{66}$  material.

## 2. Experimental procedure

### 2.1. Crystal growth and sample preparation

$\text{YB}_{66}$  single crystals have been grown by an indirect heating oating zone (IHFZ) method [7, 8, 9]. This material is a low conductivity p-type semiconductor, so that it is difficult to couple directly with induction heating of the order of hundred kHz. In the IHFZ method, specifically developed for the growth of  $\text{YB}_{66}$  single crystal, a molten zone is heated by radiation from an inductively heated tungsten ring which is situated between the molten zone and RF coil.

Unit processes for  $\text{YB}_{66}$  crystal growth begin at the synthesis of raw powder of the material, which is not commercially available. In order to keep carbon contamination level in the polycrystalline rod as low as possible, it is necessary to use carbon free components for an induction heating furnace. Because of relatively low density of polycrystalline feed rods, multi-zone pass (at least two) was necessary to achieve high quality in single crystals. For the first zone pass, the driving rates of the crystal and the polycrystalline feed rod were 25 and 45-50 mm/h, respectively. The higher driving rate of the feed rod is to compensate for the porosity of the feed rod. For the second pass, the driving rates of the crystal and the densified feed rod remain identical, 10

to 12 mm/h. The crystal and the feed rod rotation rates were 6 rpm and 0-6 rpm, respectively. A pressurized He atmosphere (0.2-0.5 Mpa) in the furnace was employed in order to reduce boron evaporation from the molten zone. In the final zone pass, a seeding process was carried out to obtain growth axis parallel to the  $[0\ 0\ 1]$  or  $[0\ 1\ 1]$  direction. The grown crystals had dimensions of about 12 mm in diameter and 60-70 mm in length. Since the crystal quality became higher with the advancing zone, the crystals used for characterization were longitudinally sliced with a diamond saw from the middle of the crystal towards the zone end leaving about 10 mm part of the zone. At the closest part of the zone end the crystal quality deteriorates during cooling process after the zone pass. Plates of  $\text{YB}_{66}$  for use as monochromators were of a rectangular shape of 10-12 mm wide, 20-25 mm long and 1 mm thick. The surfaces were parallel to  $\{1\ 0\ 0\}$  planes. The polishing process consisted of rough polish with  $\text{B}_4\text{C}$  powder followed with  $9\ \mu\text{m}$  diamond abrasive powder. After successive  $3\ \mu\text{m}$  diamond abrasive powder polishing, a final polish was performed with  $1\ \mu\text{m}$   $\text{Al}_2\text{O}_3$  abrasive powder on a tin polishing plate.

## 2.2. Characterization methods

$\text{YB}_{66}$  crystals were characterized using a variety of diffraction techniques to elucidate various growth induced defects and their location as a function of the crystal growth parameters. These techniques included white synchrotron radiation transmission and reflection topography, white beam section topography and double-crystal rocking curve measurements using both  $\text{Cu K}\alpha$  and  $\text{Mg K}\alpha$  conventional X-ray sources.

White beam topography data were collected on beamline 2-2 at SSRL, using high resolution Kodak SR5 film. The most frequently used reflections for data analysis were  $10\ 0\ 0$  for reflection topography and  $8\ 6\ 2$  and  $8\ 8\ 2$  for transmission topography. With this technique direct information about the quality of the crystals in terms of low-angle grain boundaries, dislocations, crystal lattice deformations was obtained. It also provided the detail location of these defects in the crystals, which is of interest in monochromator applications. White beam section topography provided information about deformation of crystal lattice within the bulk of crystal plates.

The rocking curves were recorded at SSRL with conventional  $\text{Cu K}\alpha$  source and double-crystal diffractometer using the silicon monochromator with  $3\ 3\ 3$  asymmetric reflection. Their FWHM values and shapes gave quantitative information about degree of deformations and mosaicity in the crystals. Crystal mapping in this case was performed by crystal translation and change of slit width. For hard X-ray rocking curve measurements,  $\text{Cu K}\alpha$  and several reflections, such as  $4\ 0\ 0$ ,  $10\ 0\ 0$ ,  $12\ 0\ 0$ ,  $14\ 0\ 0$  and  $16\ 0\ 0$  were used. In the early stage of this development, before the crystal quality improved to the point that they could be tested using soft X-ray synchrotron radiation, a double-crystal system at Lawrence Livermore National Laboratory with  $\text{Mg K}\alpha$  (1.25 keV) X-ray tube and beryl as a crystal monochromator was used to measure the rocking curve of  $\text{YB}_{66}$  [15]. Limited mapping was obtained by translation of the crystal in one

direction.

A more advanced and complete crystal quality mapping was performed with a DCD Mapper (Waterloo Scientific Inc.) at the National Institute for Research in Inorganic Materials. In this method, double-crystal rocking curves of  $\text{YB}_{66}$  10 0 0 reflection were collected using  $\text{Cu K}\alpha$  and  $\text{Si 1 1 1}$  as a first crystal in an areal grid of  $0.5 \times 0.5 \text{ mm}^2$  on a sample surface. Parameters such as full-width at half-maximum, peak intensity and peak position were recorded. The mapping of these parameters provides a quantitative measure of the crystal quality.

### 3. Experimental results

#### 3.1. Correlation of changes in $\text{YB}_{66}$ crystal growth process with characterization results

In an attempt to achieve a monochromator grade crystal quality, there were many experimental improvements introduced in the crystal growth process. Grown materials resulted from such procedure were tested with the topography and goniometry to elucidate its effect on the generation of defects. There were seven major modifications implemented. These are:

(i) *Increase of number of zone passes*: The polycrystalline feed rods have a relatively low sintered density of about 60%. Zone pass for such low density rods could not produce a high quality single crystal. The second zone pass using the rod densified by the first zone pass achieved high quality [16].

(ii) *Reduction of carbon impurity concentration*: Partition coefficient of carbon for  $\text{YB}_{66}$  is greater than unity. In the beginning the carbon impurity in the feed rods with a level of about 0.15 wt% accumulated to a level of 0.3-0.4 wt% at the initial part of the crystal by the double zone pass. This high carbon contamination could be expected to deteriorate crystal quality. Adoption of carbon free components in the furnace and low carbon boron source reduced the carbon contamination level less than 0.08 wt%.

(iii) *Upward drive*: In order to make seeding and necking of the crystal easy, upward drive was tried. In the IHFZ method, the molten zone accepts radiation only from the sides. It is almost impossible to keep the molten droplet in a stable position for seeding at the bottom of the feed rod. It is very easy to freeze the bottom of the molten droplet. On the other hand, it is rather easy to keep the molten droplet from freezing at the top of the feed rod due to convection in the droplet heating the top. Crystal #6648 was the first single crystal of relatively good quality grown by the upward drive. With this crystal, topographic and double-crystal diffraction characterizations were initiated [10, 13]. The longitudinally cut crystal, i.e., along the  $[0 0 1]$  direction, and cross-sections perpendicular to the  $[0 0 1]$  were studied. Fig. 1a - Fig. 1c show the 2 8 6 transmission topographs of three different parts of the crystal. The best quality part of this crystal was near the seed end (Fig. 1a) and was only a few mm in length. The 4 0 0 double-crystal rocking curve measured with  $\text{Cu K}\alpha$  radiation for this area had FWHM of 110-140 arcsec. In the soft X-ray energy region, the measured FWHM was about

130 arcsec, for Mg  $K\alpha$  radiation from conventional X-ray tube, which corresponds to an energy resolution of 0.4 eV. This encouraging result led to further efforts to obtain better quality crystals. However, the crystal quality deteriorated gradually away from the seed end (Fig. 1b) and then more rapidly with molten zone advancing towards the zone end, where the large number of sub-grain boundaries and strong lattice distortions were observed (Fig. 1c). The 4 0 0 rocking curves of the zone end exhibit multi-peak structure, which is typical for sub-grain boundaries. The misorientations of the order of 500-900 arcsec were obtained from the rocking curve width for Cu  $K\alpha$  and rocking curve peak position change for Mg $K\alpha$ . The reflectivities measured with Mg  $K\alpha$  varied from 0.7-2.3% dependent on positions of the crystal. It is believed that the quality deterioration was caused mainly by a concave growth interface [?]. Reversing the drive direction from upward to downward was necessary in order to change the concavity of the growth interface to a convex one.

(iv) *Downward drive*: For downward drive, because of the reason mentioned above, it is difficult to carry out seeding from the bottom of the feed rod using a thin seed crystal. Therefore, a seed crystal having the same diameter as that of the feed rod was used. In this case many sub-grains nucleated at the seeding position. After the seeding, however, the convex growth interface grew the central sub-grain gradually. Fig. 2 shows the 10 0 0 reflection topograph of a longitudinally cut piece of the crystal #6701, grown using this technique. The central part of a longitudinal section at the zone end of #6701 showed a single peak 4 0 0 Cu  $K\alpha$  rocking curve of FWHM of about 110 arcsec.

The downward drive appeared to yield high quality crystals, but the growth of the central subgrain was so gradual that high quality region at the zone end part was again very narrow. Moreover, the central part often consisted of a few sub-grains instead of single grain. Misorientations higher than 1100 arcsec were measured between each sub-grain even at the zone end. Reflectivity did not reach a value higher than 2% as measured with Mg  $K\alpha$ . The quality of each singular sub-grain was relatively high as characterized by rocking curves. Crystal quality deteriorated very rapidly off the center of the boule so that for the surface 1.5 mm radially off the center only multi-peak rocking curves were measured. Another change was necessary to obviate the multi-peak situation in the rocking curve.

(v) *Adoption of an incongruent growth*: A great advantage of the FZ crystal growth is its capability of growing crystals under an incongruent melting condition where a composition of the molten zone is different from and in equilibrium with that of the growing crystal [8]. This method can reduce growth temperature as compared with the congruent melting growth at the highest temperature [17]. In the case of YB<sub>66</sub>, the composition of the molten zone was [B]/[Y] = 40 and that of the growing crystal is about 56, which was the Y-richest composition in the homogeneity region of YB<sub>66</sub>. Crystal #6757 which is the first one grown under such an incongruent condition, is currently being used successfully as the first soft X-ray monochromator for synchrotron radiation in the energy region 1-2 keV at SSRL [6].

Actually the #6757 crystal was cut into four pairs; a pair of seed end side plates

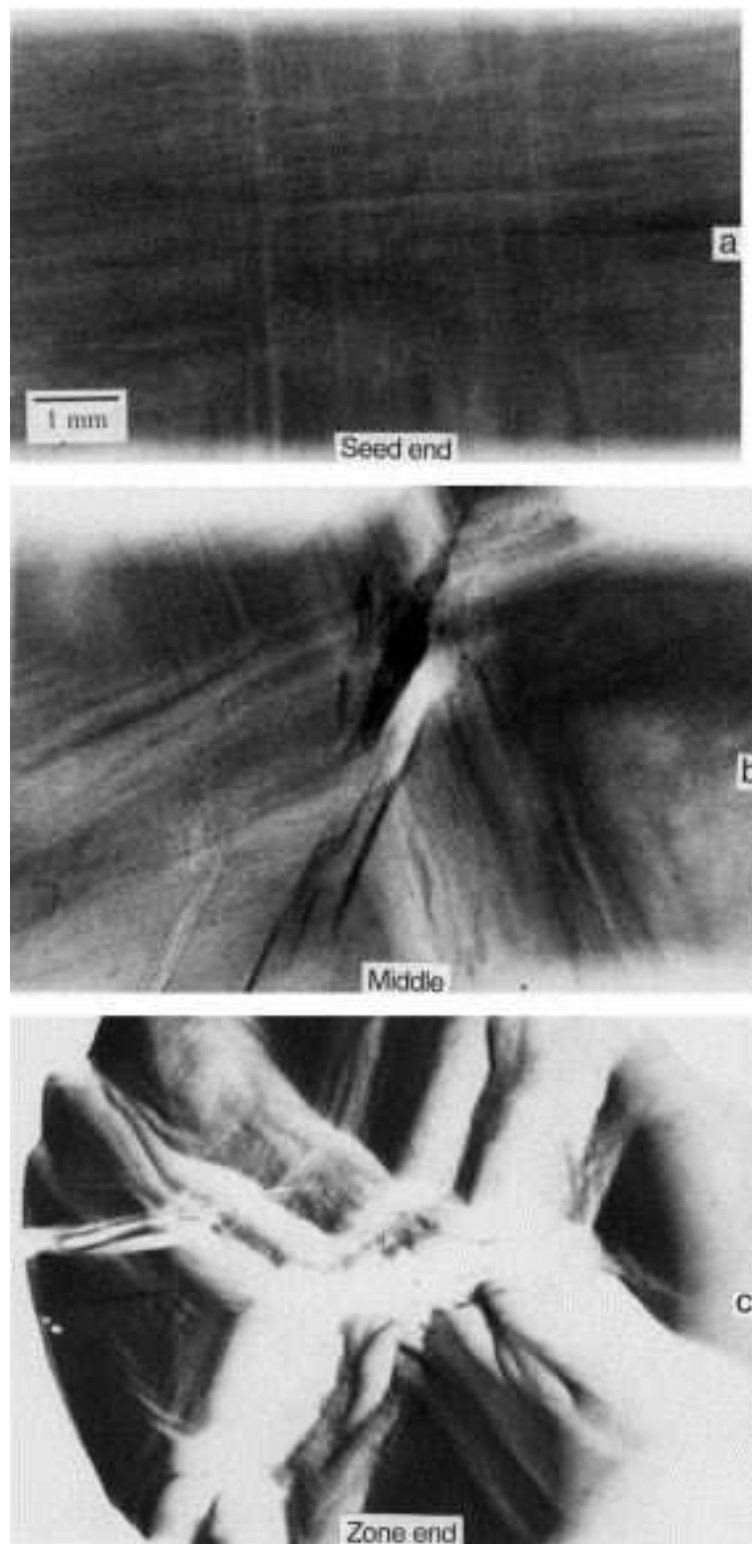


**Figure 1.** Transmission synchrotron topographs of three different cross-sectional parts of #6648 crystal grown by the upward drive procedure: (a) The seed end part, (b) the middle part and (c) the zone end part, 2 8 6 reflection at 0.9 Å wavelength.

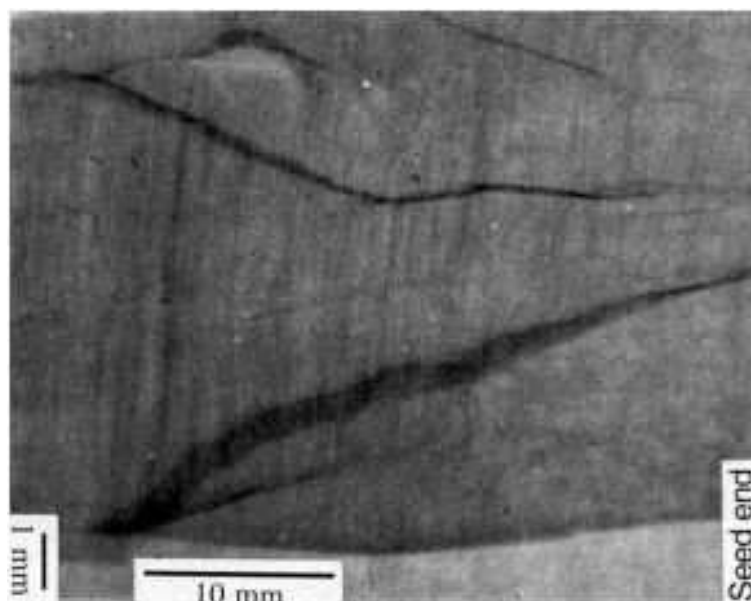


**Figure 2.** Reflection topograph of a longitudinally cut piece of the #6701 crystal grown by the downward drive method, 10 0 0 reflection at 0.81 Å wavelength. The right side corresponds to the seed end and the left side corresponds to the zone end of the crystal, respectively. The central sub-grain nucleated at the seeding position gradually grew to about one third of the crystal diameter.

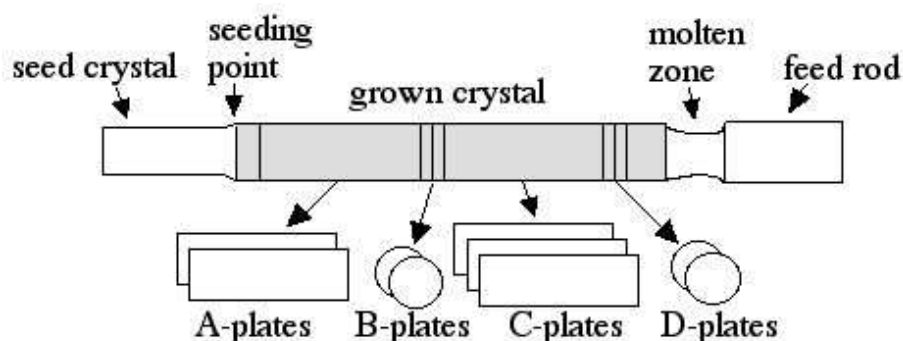


**Figure 3.** Schematic illustration for cut pieces of A, B, C and D of the #6757 crystal.

longitudinally sliced, two cross-sectional plates, another pair of zone end side plates longitudinally sliced and another two cross-sectional plates at the zone end. These parts were labelled as A, B, C, and D parts, respectively, and are illustrated in Fig. 3 where an additional C-plate is also shown. The C-pair was about 15 mm in length and one end of them was 5 mm from the zone end. In the C-plates, relatively uniform central area especially at the D-side was obtained as visible in the transmission and reflection Laue topographs shown in Fig. 4. This particular area was very critical soft X-ray monochromator applications. The incongruent growth method appears to be characteristic for the production of crystals with high quality central region radially

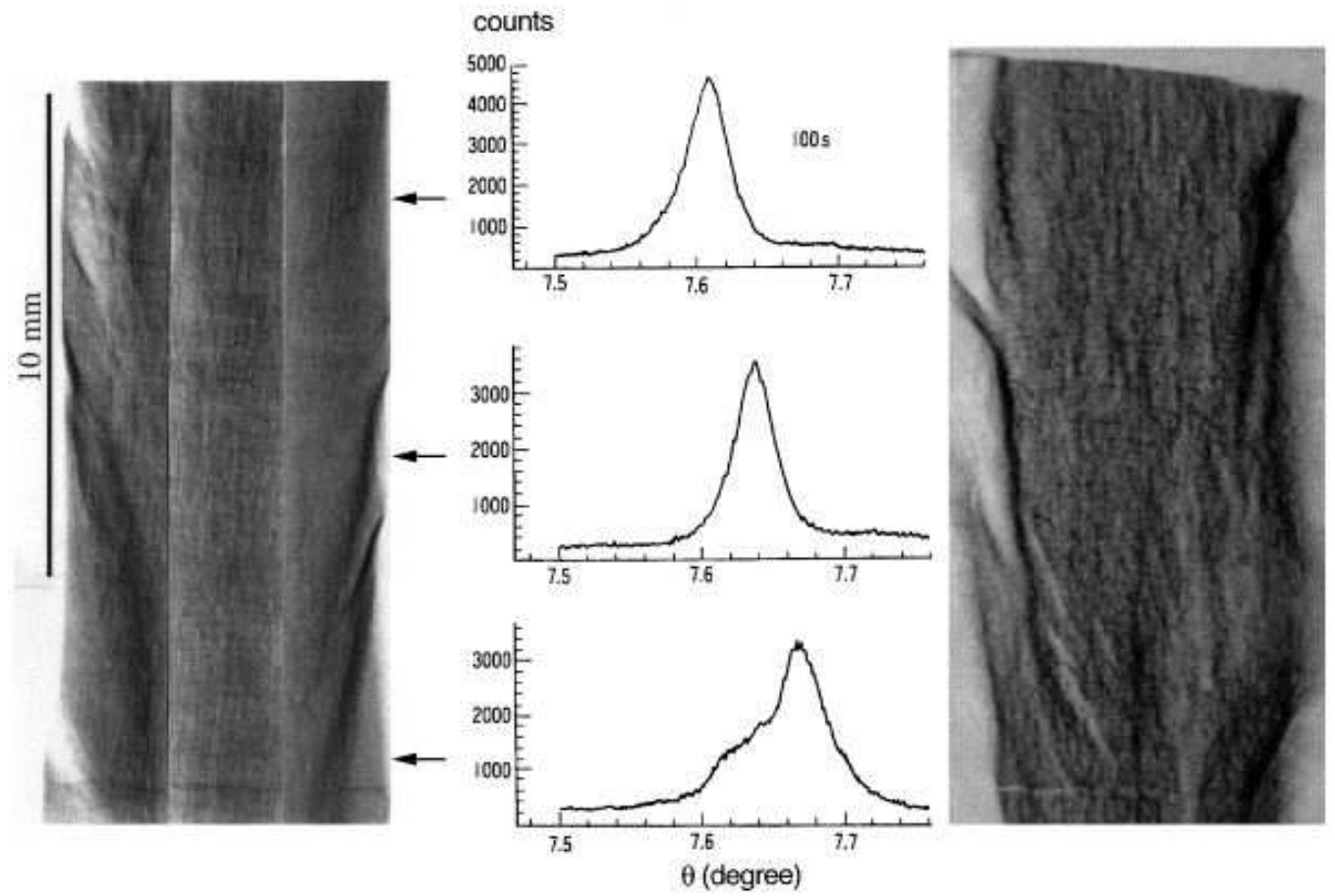


**Figure 4.** Transmission topograph (left), 2 6 8 reflection at 0.92 Å wavelength and reflection topograph (right), 10 0 0 reflection at 0.81 Å wavelength of the C-plate of the #6757 crystal incongruently grown and Cu Kα (4 0 0) rocking curves (middle) at three positions of the same plate. Top and bottom sides corresponds to D- and B-sides, respectively. (In the transmission topograph, three topographs having nearly same darkness on each part are gathered in order to give a better image through whole crystal. The two straight lines divided them do not correspond to crystal deformation of any sorts.)

out to about 13 of total crystal diameter and lower quality side regions containing some subgrain boundaries.

The rocking curve of the central part of the C-plate had FWHM of the 4 0 0 reflection of about 100 arcsec as shown in Fig. 4. This value was obtained with a horizontal slit size of 0.5 mm, that corresponded to ca 3.5 mm of illuminated crystal area. The rocking curve at the B-end side of this C-plate is wider and more asymmetric than that of the D-side, which agrees with the less uniformity observed in both topographs. The reason for this effect was caused by unexpected molten zone instability that occurred around the B-part during zone pass process.

However, it must be emphasized that this growth mode can achieve high crystal



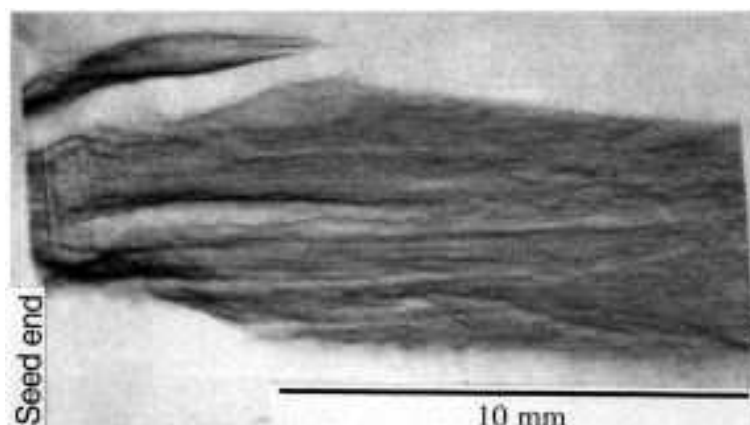


**Figure 5.** Reflection topograph of the A-plate of the #6757 crystal, 10 0 0 reflection of 0.81 Å wavelength. The left side corresponds to the seed end. The rocking curve half width at the right side (corresponds to the middle of the crystal) was comparable to those of the top two in Fig. 4.

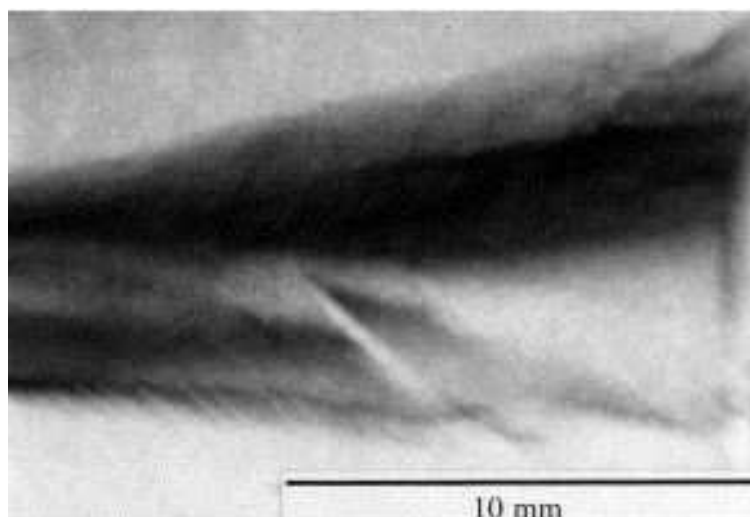


**Figure 6.** Reflection topograph, 10 0 0 reflection at 0.92 Å wavelength, of the 3rd longitudinally cut C-plate from the #6757 crystal.

quality rather rapidly than the congruent growth mode. This can be understood well from a reflection Laue topograph of the A-plate which is shown in Fig. 5. Though some nucleation of sub-grains could be observed at the seeding side, the crystal became uniform relatively soon throughout the whole observed area. In fact, the rocking curve for the B-side of this sample had a comparable FWHM value with that of the D-side of the C-crystal. That is, the incongruent growth can attain high quality much quicker than the congruent growth. However, only two parallel plates of ca 1 mm thickness could be obtained from this boule, since its quality, as mentioned before, deteriorates rapidly towards the side of crystal. In fact, the reflection topograph (Fig. 6) of the crystal cut as the third after two C-plates used as monochromators showed a relatively

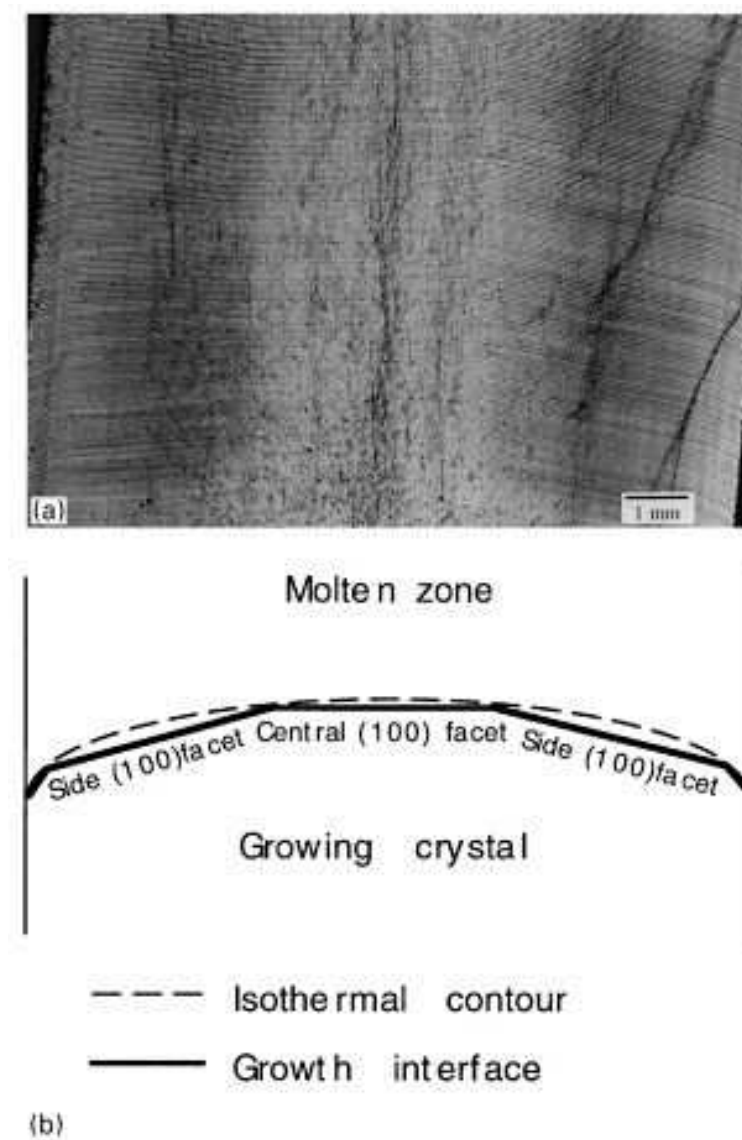


**Figure 7.** (a) Growth striation revealed by chemical etching for a longitudinal (1 0 0) section of a crystal grown parallel to the  $[0\ 0\ 1]$  direction. Two side  $\{1\ 0\ 0\}$  facets and the central  $\{1\ 0\ 0\}$  facet can be observed as schematically illustrated in (b).

poor crystal quality.

(vi)  $[0\ 1\ 1]$  growth:  $\text{YB}_{66}$  exhibits a strong tendency to facet. The  $(1\ 0\ 0)$  plane shows the strongest faceting property [18]. All crystals until recently have been grown parallel to the  $[0\ 0\ 1]$  direction. As can be seen in Fig. 7a which shows a growth striation revealed by chemical etching for a longitudinal  $(1\ 0\ 0)$  section of a crystal, there are two side  $\{1\ 0\ 0\}$  facets as well as the central  $\{1\ 0\ 0\}$  facet. These three facets roughly resemble the shape of convex equi-temperature contour by three straight lines which are schematically illustrated in Fig. 7b. The side facets are inclined towards the central facet from half to several degrees. This can be understood more clearly by a transmission Laue topograph on the cross-section D of the #6757 crystal shown

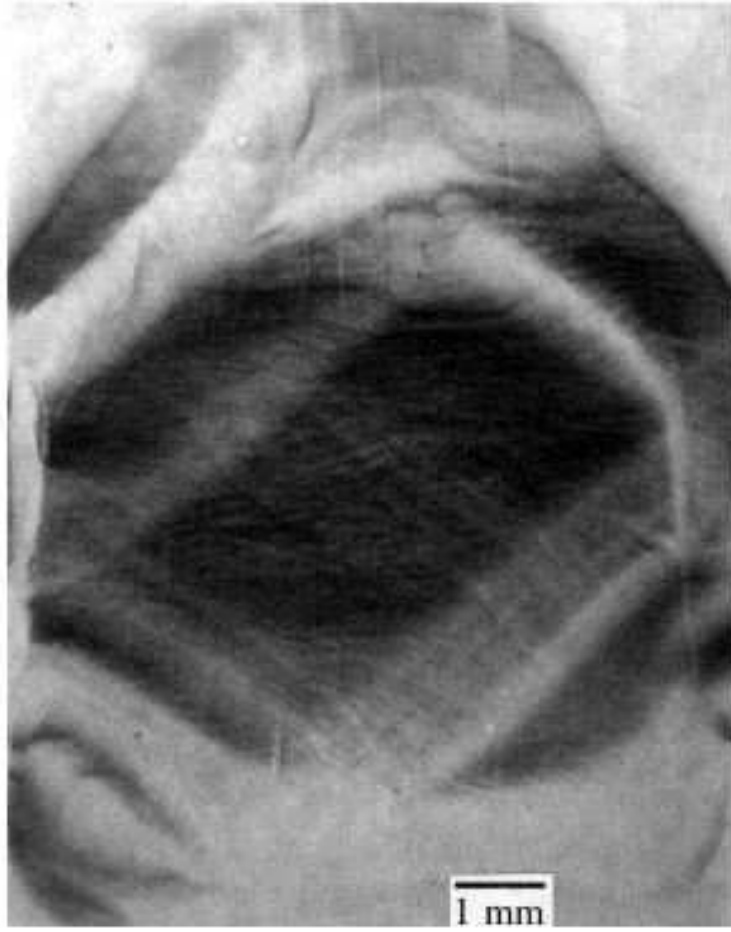


**Figure 8.** Transmission topograph of the cross-section D of the #6757 crystal, 10 0 0 reflection at 0.81 Å wavelength.

in Fig. 8. Four sub-grains surround the central sub-grain. Lattice misfit between the central facet and the side facets is a source of sub-grain boundaries incorporated into the peripheral region and only the central facet continues to preserve a high quality.

In an attempt to solve the faceting problem, crystal growth in the  $[0\ 1\ 1]$  direction was tried. For practical monochromator application of  $\text{YB}_{66}$  the  $\{4\ 0\ 0\}$  diffraction plane is used. So the surface of the monochromator must be the  $\{1\ 0\ 0\}$  plane. In order to achieve it by cutting the crystal longitudinally, growth direction must be parallel to the  $[0\ k\ l]$  direction. The faceting property of lower index planes is stronger, judging from the observation for a crystal surface grown parallel to the  $[0\ 0\ 1]$  direction, i.e., the  $\{1\ 0\ 0\}$  facets appear very sharply, then  $\{1\ 1\ 0\}$  and  $\{2\ 1\ 0\}$  sequentially follow. Growth along higher index axes may help to avoid the faceting problem present in the  $[0\ 0\ 1]$  growth.

Several crystals were grown also along a direction about  $10^\circ$  off from the  $[0\ 1\ 1]$  direction towards the  $[0\ 2\ 1]$  direction in order to avoid the  $\{1\ 1\ 0\}$  faceting. Crystals #6839 and #6840 grown by this way had FWHM of the  $4\ 0\ 0$  reflection of 70 and 86

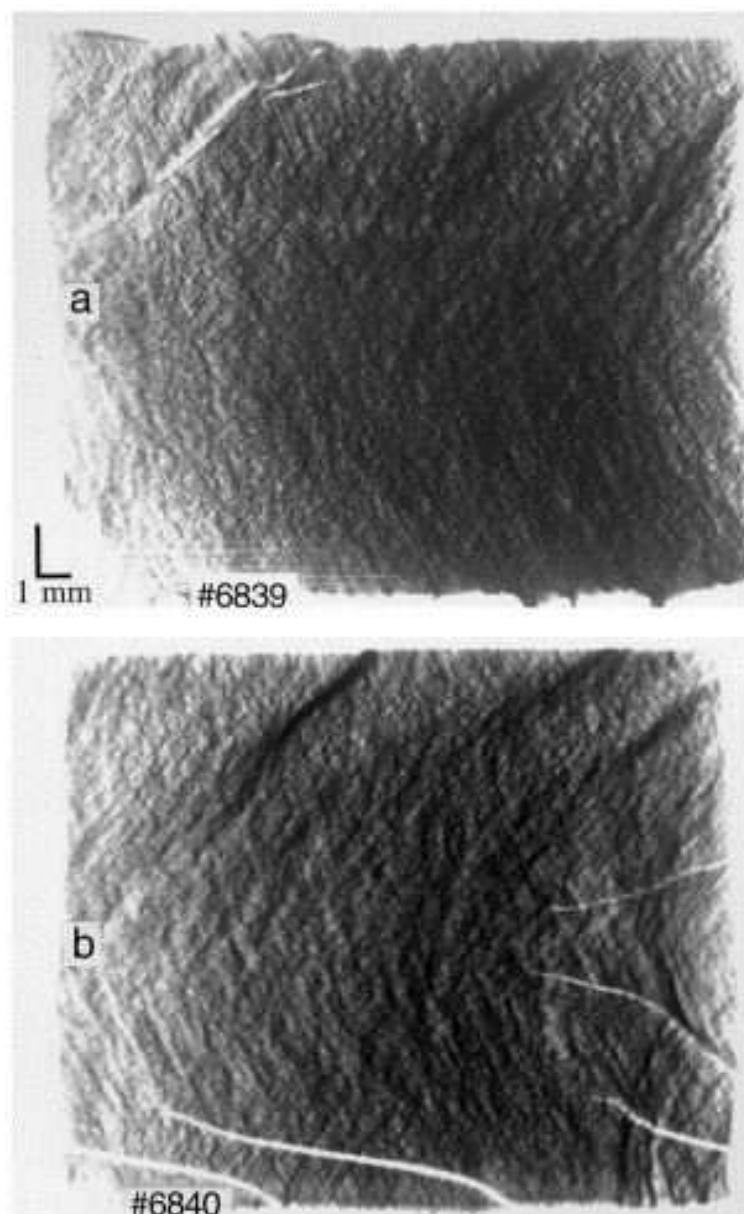


**Figure 9.** Reflection topographs of the #6839 crystal (a) and #6840 crystal (b), 10 0 0 reflection at 0.81 Å wavelength.

arcsec, respectively, in the highest quality area. These values are considerably lower than that of #6757. Reflection Laue topographs of #6839 and #6840 are shown in Fig. 9a and Fig. 9b, respectively. Mosaicity of the crystals can be seen in both figures as oblique cross hatches.

These white beam topography results for both crystals were compared with the crystal quality maps of FWHM, peak intensity and peak position for the 10 0 0 reflection. FWHM maps of the #6839 and #6840 crystals are presented in Fig. 10a and Fig. 10b, respectively. Average FWHM of #6839 is 49 arcsec and about 10% narrower than that of #6840 (58 arcsec) in the central parts of the crystals. The FWHM maps correspond

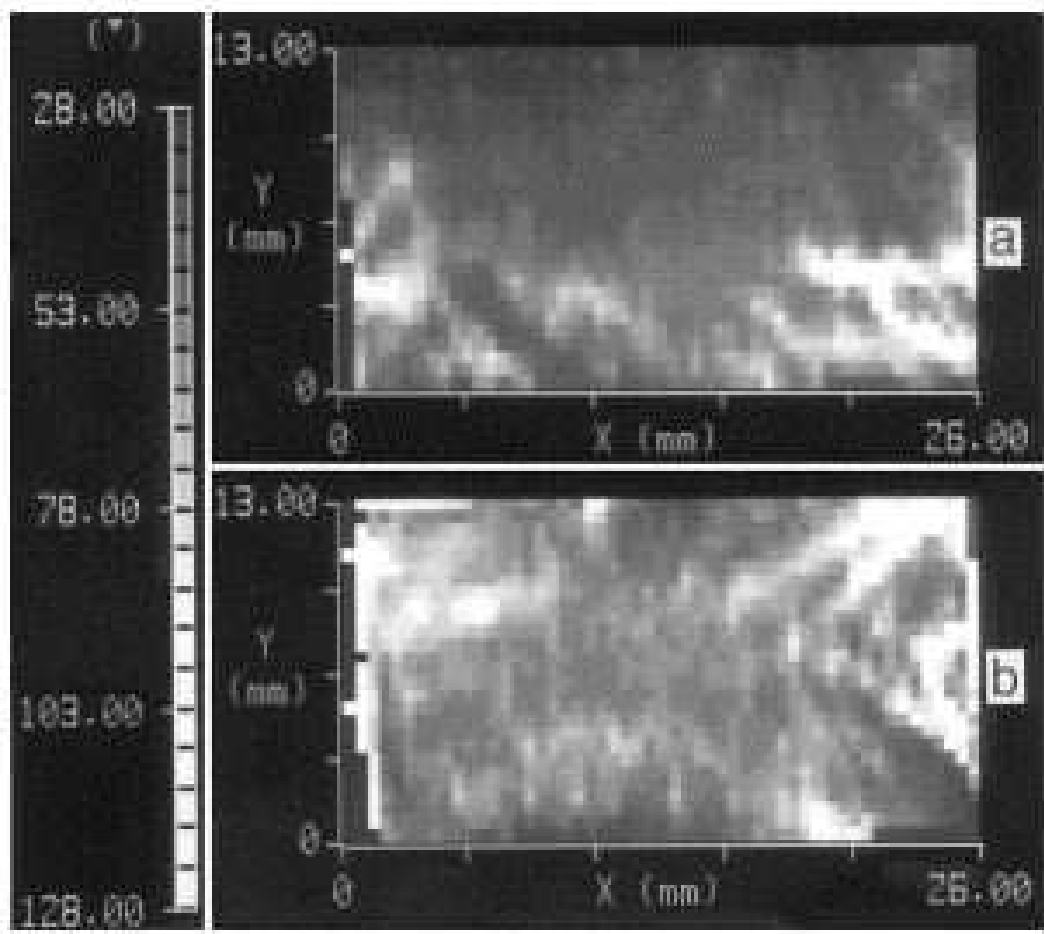


**Figure 10.** FWHM maps of the #6839 crystal (a) and #6840 crystal (b). Contrast scale is also shown for every 5 arcsec step of FWHM values which range from 28 to 128 arcsec.

well to the sub-grain boundary structure and appeared in the white beam topographs. At the sub-grain boundary region, the FWHM values became larger.

Although in the  $[0\ 1\ 1]$  growth the feature of high quality central region and side sub-grains is basically unchanged, the former region becomes wider than in the case of the  $[0\ 0\ 1]$  growth. The  $[0\ 1\ 1]$  growth seems to attain higher quality than the  $[0\ 0\ 1]$  growth judging from these results.

(vii) *Relation between heating power and crystal quality:* It is obvious that the molten zone of the floating zone crystal growth becomes unstable and drops down if excessive heating power causes the molten zone height to exceed its stability limit. However, thermal conductivity of  $\text{YB}_{66}$  is so low ( $2\text{--}3 \times 10^{-2}$  watt/cm/K) that the excessive heating power changes the shapes of the growth and melting interfaces from convex to concave more than the molten zone height. Thus the molten zone of  $\text{YB}_{66}$  FZ growth can be held without dropping down for considerably wide heating power range. On the other hand, at high heating power the molten zone vibrates, which

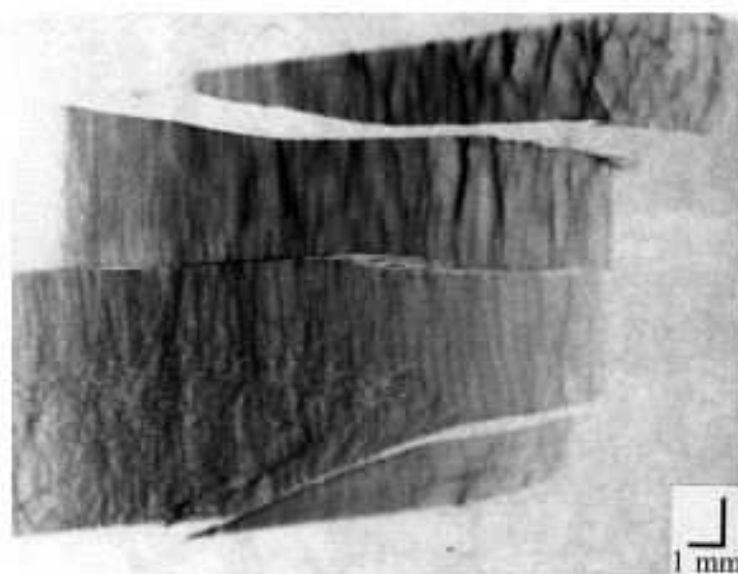


**Figure 11.** Reflection topograph, 10 0 0 reection at 0.81 Å wavelength, of an example of the #6826 crystal grown under excess heating power condition.

may be induced by a violent convection in the molten zone. This condition caused an instability of the growth interface. An example of  $\text{YB}_{66}$  crystal (#6826) grown under such condition is shown with the reflection Laue topograph in Fig. 11. Sub-grain occurrence and lattice plane undulation can be seen clearly. Evidently higher heating power worsens crystal quality. The topographs of Fig. 9a and Fig. 9b correspond to the crystal #6839 and #6840 which were grown under the lowest heating power condition and have had the highest quality in the crystals grown to date. To achieve high quality  $\text{YB}_{66}$  crystals, the heating power should be kept as low as possible.

#### 4. Discussion

Each of systematic changes adopted in a number of critical parameters associated with the growth process brought about a significant improvement in crystallographic quality of  $\text{YB}_{66}$  material. The crystals initially grown with both downward and upward movement had only small areas of high crystal quality. The appearance of large number of small and large sub-grain boundaries was typical for both processes. Rocking curve shapes, FWHM values, crystal reflectivity and overall surface deformations varied significantly through the entire sample strongly dependent on the position of the crystal. Crystal lattice misorientations of the order of 1200 arcsec and the reflectivities no higher than 2.3% were recorded. The quality of such crystals was not adequate for monochromator application.

Introduction of the incongruent growth significantly improved crystal quality to the level that they could be used successfully as functional monochromators for soft X-rays at beam line 3-3 at SSRL. In this case crystal central area, about 1/3 of the crystal

diameter, was relatively of high quality despite the fact that the rocking curve width and reflectivities were not uniform throughout the entire central section and the sides of crystal contained sub-grain boundaries. The Cu  $K\alpha$  4 0 0 rocking curves had values of the order of 100 arcsec and reflectivities in the highest quality area were 3-5%, the overall lattice misorientations measured were no more than 300 arcsec. The alignment of these crystals, however, required a beam line as flexible as JUMBO 3-3 at SSRL to avoid illuminating the low quality part of the crystal and to enable spectral scans over a wide energy range of ca 600 eV [15].

The highest quality crystals grown to date were obtained with the incongruent growth in the  $[0\ 1\ 1]$  direction. Crystals grown this way are characterized by their higher uniformity, lack of sub-grain boundaries or very small sub-grain boundaries at the sides of the crystal. FWHM values are about 20% narrower than for the incongruent growth in the  $[0\ 0\ 1]$  direction and the lattice misorientations of the crystals are 60-100 arcsec.

In order to estimate how close the present crystal quality comes to the ideal one, theoretical rocking curve widths were calculated to be 1.45, 10.8 and 34 arcsec for the energies of Cu  $K\alpha$ , 1500 and 1100 eV, respectively. The values for Cu  $K\alpha$  and 1500 eV agree well with previously calculated ones [11], but the value at 1100 eV is about 30% smaller than the previous one. The 4 0 0 Cu  $K\alpha$  rocking curve widths experimentally obtained are a factor 30-50 higher than that theoretically calculated. This is due to the mosaicity existing in these crystals. Hard X-ray measurements are especially sensitive to it, because the Bragg angle for  $YB_{66}$  is relatively small and even with the small beam size a large crystal area is illuminated. In addition, FWHM's for higher order reflections such as 10 0 0 and 16 0 0 have values nearly constant and much higher than that theoretically calculated, of factor 50 or more, which clearly indicates the presence of mosaicity in the crystals.

On the other hand, measured FWHM values at 1100 and 1500 eV seem to come closer to calculated values, i.e., they differ by a factor 3-10, because at soft X-rays energy range, rocking curves are collected from rather small area due to large Bragg angles. The beam illuminates only a small number of sub-grains or cellular cells and also X-ray penetration depth is much smaller.

In the transmission Laue topography of #6839, shown in Fig. 12, single lines that look like single dislocations could be resolved. These lines are aligned parallel to  $[0\ 1\ 1]$ . These could be large groups of dislocations rather than single dislocations, because of the strong mosaicity visible in this crystal. The nature of these lines is currently under investigation.

## 5. Concluding remarks

After numerous iterations of growth process improvements supported by feedbacks of characterization results, high quality single crystals of  $YB_{66}$  were obtained and tested as an actual optical element for monochromatization of soft X-rays of synchrotron

radiation. The highest quality crystals grown to date were obtained with the incongruent growth in the  $[0\ 1\ 1]$  direction. The existence of defects and mosaicity in these crystals did not have a big effect on monochromator resolution. The measured energy resolution of YB<sub>66</sub> in the doublecrystal mode varies typically from 0.25 eV at 1050 eV to  $\sim 1$  eV at 2000 eV [6]. Moreover, in EXAFS measurements the YB<sub>66</sub> monochromator can give  $k_{\text{max}}$  values of  $\sim 13.5\ \text{\AA}^{-1}$  for the Mg spectrum and  $\sim 11.0\ \text{\AA}^{-1}$  for the Al spectrum, respectively, which are much greater than those obtained by beryl monochromator for Mg and a quartz (10 10) monochromator for Al [13].

After the first installation of the YB<sub>66</sub> soft X-ray monochromator on BL 3-3 at SSRL in 1993, its impact on XAFS spectroscopy in 1-2 keV energy region has been well recognized. Currently, a number of synchrotron radiation facilities beside SSRL are equipped with this YB<sub>66</sub> capability: UVSOR (Okazaki, Japan), SRS (Daresbury, UK) and the number is expected to grow as the monochromator materials become commercially available [19].

## References

- [1] S.M. Richards, J.S. Kasper, *Acta Crystallogr. B* 25 (1969) 237.
- [2] P.A. Medwick, D.G. Cahill, A.K. Raychaudhuri, R.O. Pohl, F. Gompf, N. Nucker, T. Tanaka, *AIP Conf. Proc.* 231 (1990) 363.
- [3] P.A. Medwick, R.O. Pohl, T. Tanaka, in: M. Meisner, R.O. Pohl (Eds.), *Springer Series in Solid State Sciences*, vol. 112, Springer-Verlag, Berlin, 1993, p. 313.
- [4] O.A. Golikova, *Sov. Phys. Semicond.* 26 (1992) 900.
- [5] J. Wong, W.L. Roth, B.W. Batterman, L.E. Berman, D.M. Pease, S. Heald, T. Barbee, *Nucl. Instr. and Meth.* 195 (1982) 133.
- [6] M. Rowen, Z.U. Rek, J. Wong, T. Tanaka, G.N. George, I.J. Pickering, G.H. Via, G.E. Brown Jr., *Synchr. Rad. News* 6 (1993) 25.
- [7] T. Tanaka, S. Otani, Y. Ishizawa, *J. Crystal Growth* 99 (1990) 994.
- [8] Y. Kamimura, T. Tanaka, S. Otani, Y. Ishizawa, Z.U. Rek, J. Wong, *J. Crystal Growth* 128 (1993) 429.
- [9] T. Tanaka, Y. Ishizawa, J. Wong, Z.U. Rek, M. Rowen, F. Schäfers, B.R. Müller, *Jpn. J. Appl. Phys. Series 10* (1994) 110.
- [10] Z.U. Rek, J. Wong, T. Tanaka, Y. Kamimura, F. Schäfers, B.R. Müller, M. Krumrey, P. Muller, *Proc. SPIE Meeting* 1740 (1992) 173.
- [11] J. Wong, G. Shimkaveg, W. Goldstein, M. Eckart, T. Tanaka, Z.U. Rek, H. Tompkins, *Nucl. Instr. and Meth. A* 291 (1990) 243.
- [12] F. Schäfers, B.R. Müller, J. Wong, T. Tanaka, Y. Kamimura, *Synchr. Rad. News* 5 (1992) 28.
- [13] J. Wong, G.N. George, I.J. Pickering, Z.U. Rek, M. Rowen, T. Tanaka, B. DeVries, D.E.W. Vaughan, G.H. Via, G.E. Brown Jr., *Solid State Commun.* 92 (1994) 559.
- [14] J. Cerino, J. Str, N. Hower, R.Z. Bachrach, *Nucl. Instr. and Meth.* 172 (1980) 227.
- [15] J. Wong, M. Rowen, T. Tanaka, F. Schäfers, B.R. Müller, Z.U. Rek, in preparation.
- [16] T. Tanaka, S. Otani, Y. Ishizawa, *J. Crystal Growth* 73 (1985) 31.
- [17] S. Otani, S. Homma, Y. Ishizawa, *J. Crystal Growth* 126 (1993) 466.
- [18] D.W. Oliver, G.D. Brower, *J. Crystal Growth* 11 (1971) 185.
- [19] Crystal Systems Inc., Kobuchizawa 9633, Yamanashi 408, Japan.